JOURNAL OF CATALYSIS **83**, 415–427 (1983)

Effect of Preparation Methods on the Catalytic Properties of Zeolite-Supported Ruthenium in the Fischer–Tropsch Synthesis

Y. W. CHEN,[1] H. T. WANG,[2] AND J. G. GOODWIN, JR.[3]

Department of Chemical and Petroleum Engineering, University of Pittsburgh,
Pittsburgh, Pennsylvania 15261

Received December 29, 1982; revised April 26, 1983

Three preparation techniques [incipient wetness using a solution of $RuCl_3$, vapor impregnation by $Ru_3(CO)_{12}$, and ion exchange with $Ru(NH_3)_6Cl_3$] have been used to prepare NaY zeolite-supported ruthenium catalysts. The effect of these preparation methods on the activity and product selectivity of the Ru catalysts in the Fischer–Tropsch synthesis was examined at temperatures in the range of 220–320°C, a pressure of 1 atm, a CO/H_2 ratio of 1, and flow rates in the range GHSV = 1800–3600 h^{-1}. It was found that there is a good inverse correlation of turnover numbers for CO conversion to the CO/H adsorption ratio, suggesting that the relative availability of adsorbed H_2 and CO determines catalyst activity during reaction. Selectivity in the Fischer–Tropsch synthesis was greatly influenced by the preparation method and metal loading. Catalysts prepared by incipient wetness produced mainly methane. Catalysts prepared by vapor impregnation had the best selectivities for higher hydrocarbons and olefins even though they had the smallest average Ru particle sizes. The observed changes in adsorption, activity, and selectivity with preparation method appear to result from differences produced in metal location in/on the zeolite, metal particle size, and zeolite–metal interactions.

I. INTRODUCTION

Ruthenium has been recognized as one of the best catalysts for the Fischer–Tropsch (FT) synthesis (*1*). It has the ability to produce significant amounts of higher hydrocarbons even at a pressure of only 1 atm. In addition, it is considerably easier to reduce than other FT catalysts, such as Fe and Co, and is not converted to a carbide under FT reaction conditions. The use of zeolite supports for FT synthesis is of particular interest since these supports offer several advantages over conventional supports, such as: (i) ability to maintain high metal dispersion, (ii) metal–zeolite interactions, (iii) bifunctional catalysis, and (iv) shape selectivity.

Various preparation techniques exist which enable one to prepare zeolite-supported metals having different physical and chemical properties. This paper reports on an investigation into the effect of these techniques on the catalytic properties of NaY-supported Ru for CO hydrogenation.

II. EXPERIMENTAL

Materials. Synthetic zeolite NaY, $RuCl_3 \cdot 1.5H_2O$, $Ru(NH_3)_6Cl_3$, and $Ru_3(CO)_{12}$ were obtained from Strem Chemicals, Inc. All gases used were UHP grade from Air Products.

Preparation and pretreatment. Three preparation techniques, incipient wetness (I.W.), ion exchange (I.E.), and vapor impregnation (V.I.), were used to introduce Ru on or into the NaY zeolite support. The incipient-wetness catalysts were prepared from $RuCl_3 \cdot 1.5H_2O$ dissolved in distilled water at a concentration sufficient to yield the proper metal loading when impregnating each gram of the support with 0.7 cm^3 of solution. After the impregnation, the samples were dried overnight in air at 40°C.

---

[1] Current address: SRI International, Menlo Park, California.

[2] Department of Chemistry.

[3] To whom all correspondence should be addressed.

0021-9517/83 $3.00

For preparing the ion-exchanged catalysts, $Ru(NH_3)_6Cl_3$ was dissolved in a weakly acidic hydrochloride solution (pH 4.5). This solution was then mixed with NaY zeolite and stirred continuously for 50 h at ambient temperature. Excess solution was used to maintain an approximately constant pH during ion exchange. After the ion-exchange reaction, the catalysts were filtered and washed several times in deionized water and dried in air overnight at 40°C.

The vapor-impregnated catalysts were prepared via the vapor phase of $Ru_3(CO)_{12}$. NaY zeolite was calcined *in vacuo* at 450°C to remove water. The impregnation then took place in an evacuated, sealed Pyrex cell held at a temperature of 80°C. This temperature ensured that the vapor pressure of $Ru_3(CO)_{12}$ was high enough for reasonably rapid adsorption on the zeolite but not high enough to cause decomposition of the carbonyl. A more detailed procedure is given elsewhere (*2, 3*).

After preparation, catalysts prepared by incipient wetness were reduced in flowing hydrogen by heating to 420°C at 0.5°C/min and holding at that temperature for 2 h. The ion-exchanged and vapor-impregnated catalysts were decomposed slowly under vacuum (ca. 3×10^{-7} Torr) by heating to 420°C (0.5°C/min) and holding for 2 h. The catalysts were then reduced in pure hydrogen at 420°C for 2 h.

Characterization. The reduced samples were characterized by atomic absorption, infrared spectroscopy, and H_2 and CO chemisorption measurements. The Ru metal loadings of the catalysts were determined by a Perkin–Elmer 380 atomic absorption spectrophotometer using the method of Fabec (*4*).

The gas chemisorption measurements were made at ambient temperature in a glass adsorption system capable of achieving a vacuum of ca. 3×10^{-7} Torr. The initial point on the isotherm required 1 day for equilibrium. Equilibrium was attained for each additional point of the first isotherm and usually required 2–4 h. Total chemisorption of hydrogen or carbon monoxide was determined by extrapolation of the linear part of the first isotherm to zero pressure, corresponding to the method described by Benson and Boudart (*5*) and Wilson and Hall (*6*). A second isotherm was measured after evacuation of the sample for 2–3 min following the first isotherm. The second isotherm provided a measure of the reversibly bound hydrogen or carbon monoxide (both chemisorbed and physisorbed). The difference between the two isotherms gave the amount of irreversibly chemisorbed hydrogen or carbon monoxide.

Infrared spectroscopy was used to study CO adsorption on Ru. The ir cell was constructed of Pyrex and had KCl windows. The cell had vacuum stopcocks at both ends to provide gas flow in and out. The catalyst was ground slightly in an agate mortar and then compressed under 3×10^4 psi into a selfsupporting disk having a diameter of 2.5 cm and a weight between 30 and 50 mg. Following catalyst pretreatment and adsorption of CO, spectra were recorded at 25°C, using a Perkin–Elmer 683 grating infrared spectrophotometer, in the range 1500–2500 cm^{-1} with a resolution of 2 cm^{-1}.

Fischer–Tropsch. Kinetic measurements were made at 1 atm total pressure using a $\frac{3}{8}$-in. stainless-steel tube reactor containing approximately 0.5 g of catalyst. The catalyst particles were sieved and only 100–120 mesh were used. The reactant gases used were H_2 (99.999%), He (99.997%), and a H_2/CO mixture ($H_2/CO = 1$, 99.9% pure), which were purified by passing through drierite and 5-Å molecular sieve traps to remove water and metal carbonyl contaminants. Prior to passage through the molecular sieve trap, the hydrogen was passed through a Deoxo unit to react any oxygen to water. The flow rate of each gas was controlled by a micrometering valve and measured by a rotameter. The product gas was transferred from the reactor to the sampling valve of the gas chromatograph via a heated transfer line and was analyzed by a Perkin–

Elmer Sigma 1 gas chromatograph. Products were separated using a 6 ft. × $\frac{1}{8}$-in. stainless-steel column packed with Porapak Q and were detected by TCD. A 0.5-cm^3 gas sample was injected into the column while its temperature was held at 50°C for 2 min. The column oven was then temperature programmed at 15°C/min to 180°C. The hydrogen bracketing technique, which gave the catalyst a 40-min H_2 exposure after every kinetic measurement, did an exceptionally good job of maintaining a clean Ru surface and giving reproducible results. In order to make sure that there was no hydrocarbon produced due to the mixing of pure H_2 and the reaction mixture by gaseous diffusion during the initial period of each reaction run, both flows were separated by a short flow of He. The CO conversion was kept below 5% to minimize the effects of heat and mass transfer and secondary reactions.

III. RESULTS AND DISCUSSIONS

H_2 and CO Chemisorption

In recent reported studies, Ru metal surface areas and particle sizes have been measured by selective gas adsorption, X-ray line broadening, electron microscopy, and related techniques. However, when high dispersions of Ru or any other metals are present in supported metal catalysts, it becomes impossible to use X-ray line broadening and exceedingly difficult to use electron microscopy methods for determination of catalyst dispersion. Also, H_2 chemisorption may not be a reliable for characterization due to the suppression of chemisorption on electron-deficient Ru (*7*). CO chemisorption is not typically an accurate method for characterization because the stoichiometry may change as the Ru particles become smaller (*8*). In addition, suppression of H_2 and CO chemisorption on SMSI catalysts is known to occur (*9*). However, even with all the possible difficulties, H_2 chemisorption still remains the best overall method to determine Ru metal surface area in highly dispersed Ru catalysts.

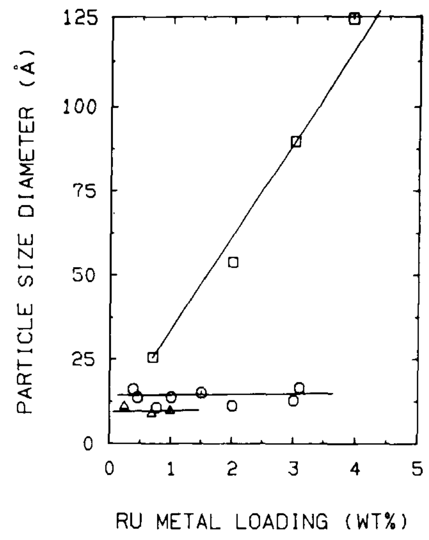

FIG. 1. Effect of metal loading on average Ru particle diameter. (□) Incipient wetness (I.W.). (○) Ion exchange (I.E.). (△) Vapor impregnation (V.I.).

In this study, the Ru surface areas were calculated from the hydrogen adsorption measurements, assuming a stoichiometry of $H_{irr}/Ru = 1$ and an average Ru area of 8.17 Å^2 (*10*). The average Ru crystallite sizes, d, were calculated using the relationship $d = \frac{5}{S \cdot \rho}$, where ρ is the density of the metal, S the surface area of Ru per gram of Ru, and the assumption is made that the particles are cubes of edge size, d, with five sides exposed to the gas phase. The resultant relationships between Ru metal loading and average particle size for Y zeolite-supported Ru prepared by different methods are given in Fig. 1. The average particle size for catalysts prepared by ion exchange was found to be independent of Ru concentration (below 3 wt%) and had values between 1 and 1.5 nm, about the size of the zeolite supercages. In contrast to the ion-exchanged catalysts, catalysts prepared via vapor impregnation by $Ru_3(CO)_{12}$ had average particle diameters of 1 nm, which were also independent of metal loading. The average particle size for the catalysts prepared by incipient wetness using an aqueous solution of $RuCl_3$ was found to vary linearly with Ru metal loading. The Ru^{+3} in the $RuCl_3$ solution used was probably in its hydrated form and, thus, too bulky to enter the zeolite pores. Most of the Ru, therefore, ended up on the limited external surface of the zeolite granules in these catalysts. Consequently, an increase in metal loading resulted in an increase in metal sintering due to its high concentration on the external zeolite surface.

The reduction of ion-exchanged RuY zeolite samples has been studied by several researchers (*11–15*). Most of these researchers have agreed that when an ion-exchanged sample is evacuated and heated slowly to 400°C prior to H_2 reduction, the average Ru particle size is ca. 1 nm. However, when H_2 is present during the dehydration procedure, the average particle size is ca. 2 nm. Our results are in agreement with these conclusions.

Some of the average particle sizes for the ion-exchanged catalysts in this study were larger than the free diameter of the zeolite supercages. These results can be rationalized in two ways. The first explanation, proposed by Verdonck *et al.* (*15*), involves the localized destruction of the lattice by H_2O to form cracks and holes. Filling of these voids by Ru metal could result in average particle sizes greater than the free diameter of zeolite. The second explanation, suggested by Gustafson and Lunsford (*12*), is that in the presence of hydrogen the mobility of Ru is increased resulting in an agglomeration of the metal in several adjacent supercages such that the particles are connected through the 12-membered windows. Based on earlier TEM results (*16*), most of the Ru is inside the zeolite framework and the largest particles are concentrated on the external zeolite surface. The presence of even a relatively few large particles is able to significantly increase the average particle size calculated.

In our study of the Ru/NaY catalysts prepared from $Ru_3(CO)_{12}$, all the average particle sizes at different metal loadings were found to be exclusively around 1 nm. The differences in average particle size found for the ion-exchanged and the vapor-impregnated catalysts may be due to one or both of the following explanations. (i) The presence of residual water in ion-exchanged catalysts results in a bimodal distribution (*15*). Since the zeolite is precalcined in a vacuum before introducing the Ru in the vapor-impregnated catalysts, less residual water is present during decomposition and reduction than in the ion-exchanged catalysts. The Ru remains highly dispersed in the supercage and, hence, produces a more monodispersed system. (ii) The greater concentration of Na in the vapor-impregnated catalysts results in a lower acidity for the zeolite, thereby suppressing interactions between the oxygen atoms of the zeolite and the ruthenium. For ion-exchanged catalysts the Na atoms have been exchanged with $Ru(NH_3)_6^{3+}$ cations during preparation. Upon reduction, the zeolite is gradually transformed into a partial hydrogen zeolite having a strong oxidizing agent (–OH group). The possible existence of metal–support interactions might cause the ruthenium to be in a higher oxidation state than the presumed value of zero. Evidence for an interaction between the oxygen atoms of alumina and ruthenium has been presented by Kellner and Bell (*17*) using infrared spectroscopy and Clausen and Good (*18*) using Mossbauer spectroscopy. Electron-deficient Pd, resulting from interaction with OH groups in NaY, has also been reported (*19*). Formation of electron-deficient surface species could suppress hydrogen adsorption to a certain extent, since highly electron-deficient metals do not appreciably interact with hydrogen (*20*). This would result in overestimation of the average particle size in the ion-exchanged catalysts.

Comparing the stoichiometry of irreversible CO chemisorption to that of H_2 shows some very interesting differences (see Fig. 2). The CO/H ratio (molecule of CO per atom of hydrogen strongly adsorbed) has a

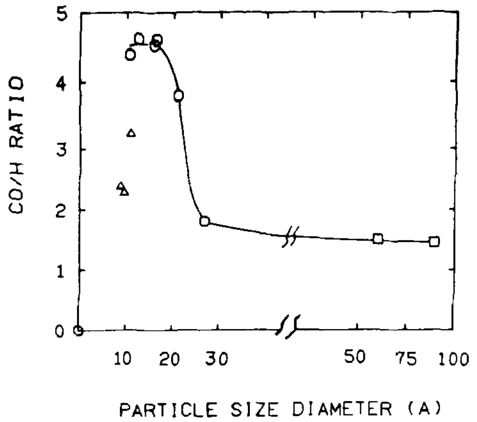

FIG. 2. Effect of average Ru particle size on CO/H adsorbed ratio. (□) I.W. (○) I.E. (△) V.I.

value of 2–3 for vapor-impregnated catalysts, while the CO/H ratio has a value of 4–5 for ion-exchanged catalysts having average Ru particle diameters less than 1.6 nm. This ratio decreases rapidly as particle size increases. The CO/H ratio for the incipient-wetness catalysts is independent of average particle size in the range above 5 nm and has a value of about 1.5. CO/H ratios greater than unity, in the absence of H_2 chemisorption suppression, imply multiple CO chemisorption to form surface species of the form $Ru(CO)_2$, $Ru(CO)_3$, and even $Ru(CO)_4$ (*21*). It can be surmised that multiple chemisorption should take place on low coordinated metal surface sites. As the particle size increases, the fraction of surface atoms of low coordination number decreases (*22*). This explains the decrease in the CO/H ratio with increasing average particle size.

The difference in CO/H ratios for ion-exchanged and vapor-impregnated catalysts having similar dispersions is probably due to metal–zeolite interactions. Based on ir results, it appears that Ru metal in ion-exchanged catalysts is probably more electron-deficient than Ru in vapor-impregnated catalysts (*24, 25*). This would result in some hydrogen suppression for the ion-exchanged catalyst. Indeed, it has been found (*23*) that there is a measurable amount of hydrogen suppression for the ion-exchanged Ru/NaY catalysts. However, suppression of CO chemisorption appears not to be significant. Therefore, the CO/H chemisorption ratios for the ion-exchanged catalysts are higher than those for the vapor-impregnated catalysts with the same metal dispersions.

Infrared Spectroscopy

Carbon monoxide chemisorption on supported ruthenium has been extensively studied by ir (*24–31*). The ir bands observed have not yet been completely assigned. However, most researchers (*31–35*) agree that smaller metal particles are less thoroughly reduced or are more modified by the proximity to the structural oxygen of the oxide support. As can be seen in Fig. 3, CO chemisorbed on the vapor-impregnated catalyst absorbs at lower wavenumbers than that on the ion-exchanged catalysts. The difference in the wavenumbers reflects differences in the ruthenium particle sizes and quite likely the effect of the zeolite on the electronic structure of the metal particle (*2, 24, 25*). Reduction of Ru has been shown to produce a decrease in the CO vibrational frequency, corresponding to a de-

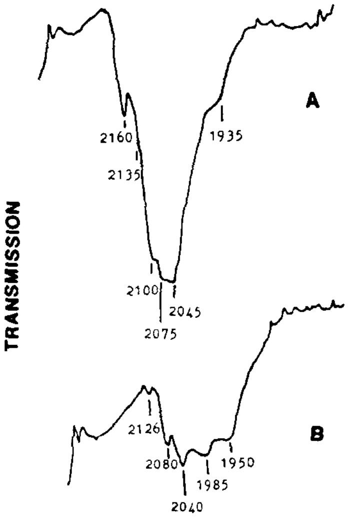

FIG. 3. Infrared spectra of CO on Ru/NaY catalysts. (A) 3% Ru/NaY (I.E.). (B) 1% Ru/NaY (V.I.).

crease in electron deficiency of the metal atoms (*26*). In an ir study of Pd supported on NaY, Chukin *et al.* (*19*) found higher frequencies than normal for CO adsorbed on reduced Pd. They ascribed this result to the interaction of the metal with strongly acidic OH groups via a donor–acceptor mechanism.

Considering both the chemisorption and ir results, it is possible that, for ion-exchanged catalysts, partial migration of free electrons from metal atoms to the proton of the strongly acidic OH groups results in the formation of a charge-transfer complex:

$$\text{Ru}\overset{\delta+\ \delta-}{\text{-------}}\text{H–O} < \text{zeolite}$$

The presence of Na^+ cations in vapor-impregnated catalysts neutralizes the strongly acidic sites:

$$\text{Ru---Na–O} < \text{zeolite}$$

and results in less interaction of the Ru with the zeolite.

The electron-deficient character of Ru for the ion-exchanged catalysts should be more than that for the vapor-impregnated catalysts. Although we are still not able to obtain CO peaks with ir for the incipient-wetness catalysts due to low Ru surface area and ir opacity of the samples, the electronic state of the Ru should be the same as bulk metal due to its large particle size and location primarily on the external zeolite surface. ESCA studies of a Ru/NaY catalyst prepared by the incipient-wetness method support this idea (*36*).

Reaction Studies

All fresh, reduced catalysts were given the pretreatment described earlier. The primary hydrocarbon products produced under all reaction conditions were α-olefins and normal paraffins. The oxygen released in conjunction with the synthesis of hydrocarbons appeared as water and small amounts of carbon dioxide. Trace amounts of methanol were also detected at low temperatures. The term "percentage total conversion of CO" refers to the conversion of CO to hydrocarbons through pentane and to CO_2. All turnover numbers were based on irreversible hydrogen chemisorption on the fresh catalysts. The steady state refers to a time frame of about 30–200 min after the start of the reaction. All designated initial reaction data were taken 5 min after the start of the reaction. By using a hydrogen-bracketing technique, activities were reproducible to within a few percent after the catalysts became stabilized. Maintaining the catalysts in hydrogen for prolonged periods was also determined to have no effect on catalyst activity.

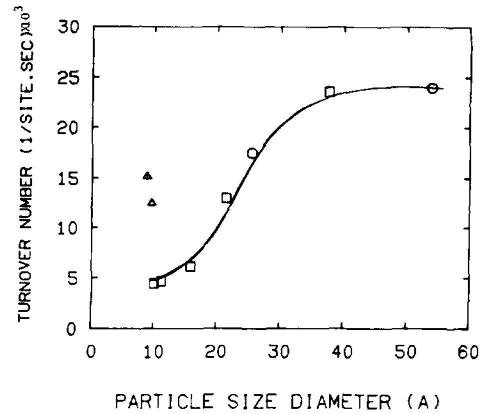

FIG. 4. Particle size effect on turnover number over Ru/NaY (reaction conditions: 250°C, 1 atm, H_2/CO = 1, GHSV = 1800). (□) I.E. (○) I.W. (△) V.I.

Particle size effects. As can be seen in Fig. 4, the turnover number of the ion-exchanged Ru catalysts was found to increase with increasing average metal particle size in the range of 1 to 3 nm. For the incipient-wetness catalysts, turnover number was constant as average particle size varied above 3 nm. A smooth curve can in fact be fit to the points from both the ion-exchanged and incipient-wetness catalysts. Selectivity for methane decreased significantly with increasing metal loading for the ion-exchanged catalysts (see Fig. 5). This was less true for the catalysts prepared by the incipient-wetness technique, which had an anomalously high methane selectivity. King (*37*) also found the latter result for

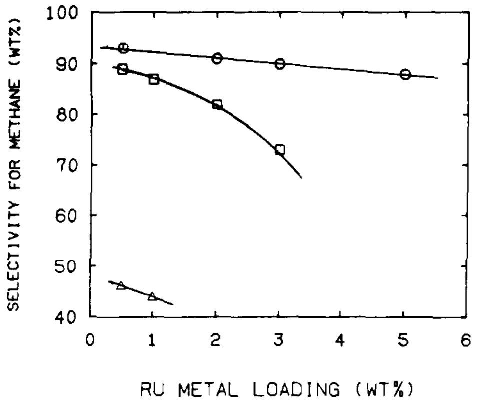

FIG. 5. Effect of Ru metal loading on the selectivity for methane (reaction conditions: 250°C, 1 atm, $H_2/CO = 1$, GHSV = 1800). (□) I.E. (○) I.W. (△) V.I.

unsupported Ru. ESCA studies have indicated that catalysts prepared by incipient-wetness method have the same properties as bulk Ru (*36*). Catalysts prepared by the vapor-impregnation method, however, exhibited greater selectivities for C_2–C_4 olefins and higher hydrocarbons than the other catalysts. In addition, their turnover numbers were much greater than those of ion-exchanged catalysts having similar dispersions of Ru.

The trend of decreasing turnover number with decreasing particle size in the range of 1–4 nm is in agreement with the data of Jacobs (*38*) for Ru/NaY and King (*37*) for Ru/Al_2O_3 and Ru/SiO_2, both data sets being over smaller ranges of particle size than the one of this study. Moreover, they were not able to prepare catalysts having average particle sizes less than 1 nm. For the sake of comparison with the present results for ion-exchanged and incipient-wetness catalysts, the results reported by Kellner and Bell (*33*) for Ru/Al_2O_3 have also been replotted in Fig. 6. It is evident that the data follow similar trends and that the slopes of straight lines fitted to each data set are nearly identical. We did not find the sharp decrease in activity for the highly dispersed Ru catalysts (% dispersion >75) reported by Kellner and Bell (*33*).

When one compares the CO/H ratios for irreversible chemisorption at 25°C for the various catalysts (Fig. 2) to their turnover numbers (Fig. 4) one finds a good inverse correlation: the greater the CO/H ratio for a given catalyst, the lower its turnover number for CO conversion. This result suggests that, under reaction conditions, hydrogen may possibly compete more successfully with CO for adsorption sites on vapor-impregnated catalysts than on ion-exchanged catalysts having similar dispersions. Such an effect would lead to the expectation that higher specific activities should occur on the vapor-impregnated catalysts, which is in fact the case. However, contrary to what would be expected, the selectivity for methane was much less.

Jung (*39*) and Bartholomew *et al.* (*40*) have reported that the larger the CO/H adsorption ratio on a catalyst, the higher its selectivity to C_2^+ hydrocarbons. They hypothesized that small metal crystallites

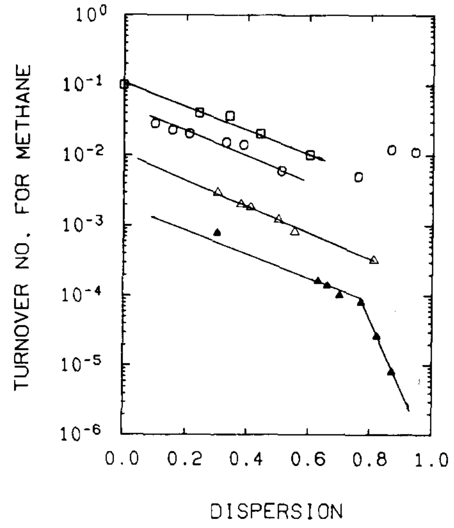

FIG. 6. Effect of dispersion on the specific activity for methane over supported Ru catalysts.

Catalyst	T (°K)	P (atm)	H_2/CO	Source
(□) Ru/Al_2O_3	523	4	2	King (*37*)
(○) Ru/NaY	523	1	1	This study
(△) Ru/Al_2O_3	498	10	3	Kellner and Bell (*33*)
(▲) Ru/Al_2O_3	478	1	2	Kellner and Bell (*33*)

TABLE 1

Effect of Preparation Methods on Isobutane Formation at 250°C

Ru/NaY catalyst	Preparation method	$\frac{iC_4}{\text{total } C_4}$ (wt%)
2%	Incipient wetness	0
4%	Incipient wetness	0
0.5%	Ion exchange	ca. 14
3%	Ion exchange	18
0.5%	Vapor impregnation	0
1%	Vapor impregnation	0

which interact strongly with the support produce hydrogen-poor hydrocarbons (compared to methane) simply because the crystallite surfaces during reaction are deficient in hydrogen. Our results did not indicate for NaY-supported Ru any such relationship between selectivity and CO/H adsorption ratio. However, it was found that the selectivity is a function of both the preparation method and the metal loading, as reported by King (*37*). More surprisingly, the vapor-impregnated catalysts were very active and produced larger amounts of higher hydrocarbons than the other catalysts. This finding does not support the particle-size-dependent reaction mechanism proposed by Nijs and Jacobs (*41*).

Significant amounts of isobutane were also observed for the ion-exchanged catalysts but were absent for the vapor-impregnated ones (*42*) (see Table 1). In the ion-exchanged catalysts, Na^+ cations have been replaced by trivalent $Ru^{3+}(NH_3)_6$. Following decomposition and reduction, three Brønsted acid sites will be produced for each Ru atom reduced. The isobutane formation would appear to be due to the presence of these Brønsted acid sites in the ion-exchanged catalysts following reduction, which produces bifunctional catalytic properties.

It has been found that the catalytic behavior of vapor-impregnated Ru catalysts depends strongly on the level of CO conversion (*43*). Amelse *et al.* (*44*) found the same result for iron alloy catalysts and discovered that this result correlates to a high activity for the water–gas shift reaction. Those catalysts having the higher water–gas shift activities produced the higher olefin selectivities and also had greater abilities for the incorporation of olefins into the growing chains. The dependence of catalytic behavior for the vapor-impregnated catalysts on CO conversion seems to be similarly correlated to a high activity for the water–gas shift reaction. For zeolite-supported Ru, it has been found that the lower the acidity the higher the activity in the water–gas shift reaction (*37*). The vapor-impregnated catalysts would obviously have the lowest acidity.

Reaction temperature effects. As can be seen in Figs. 7 and 8, the turnover number for CO and the methane selectivity increased with increasing reaction temperature for all the catalysts. However, the selectivity for methane increased more significantly for the ion-exchanged catalysts. The olefin fraction in C_2–C_4, on the other hand, decreased with increasing reac-

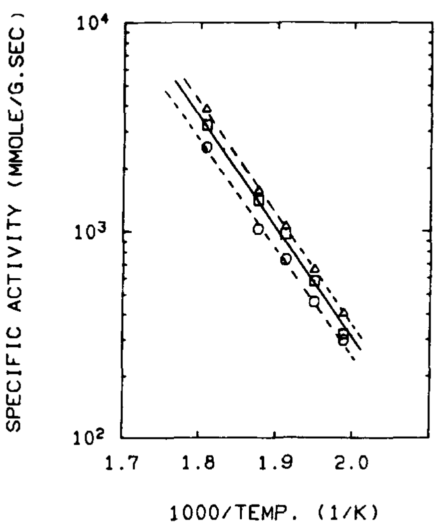

FIG. 7. Arrhenius plot for zeolite-supported Ru catalysts. (□) I.E. (3% Ru). (○) I.W. (2% Ru). (△) V.I. (1% Ru).

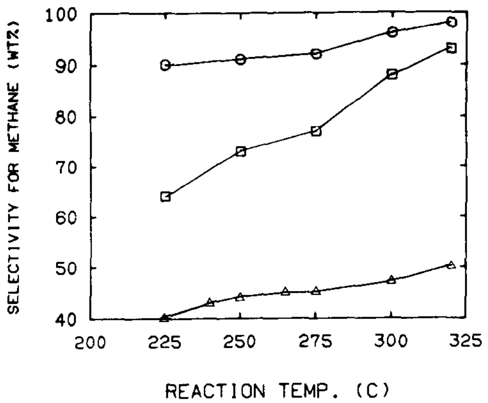

FIG. 8. Reaction temperature effect on selectivity for methane (reaction conditions: 1 atm, $H_2/CO = 1$, GHSV = 1800). (□) I.E. (○) I.W. (△) V.I.

tion temperature in all cases (see Fig. 9). This is consistent with results cited in the literature (*38*, *45*, *46*).

The selectivity changes observed on variation of the reaction temperature are not just due to thermodynamics. It can be shown that the Gibb's free energies of reaction for the formation of higher molecular weight hydrocarbons in the FT synthesis are more negative and decrease more rapidly with decreasing temperature than those of lower molecular weight hydrocarbons for FT conditions (220–320°C). Thus, the formation of a smaller fraction of CH_4 as the temperature is decreased would be expected. However, the formation of paraffins are thermodynamically favored at FT temperatures. Since the relative differences between the Gibb's free energies of the paraffins and olefins become less as temperature decreases, it has been suggested that this should result in an increase in the olefin fraction as reaction temperature is decreased (*47*). However, such an explanation cannot possibly explain the formation of olefin fractions which exceed those of the paraffins. The greatest variance in the olefin fraction probably results from differences in various kinetic steps. It is suggested that olefins are primary products in FT and their fraction decreases with increasing temperature due to an increase in hydrogenation activity (*48*).

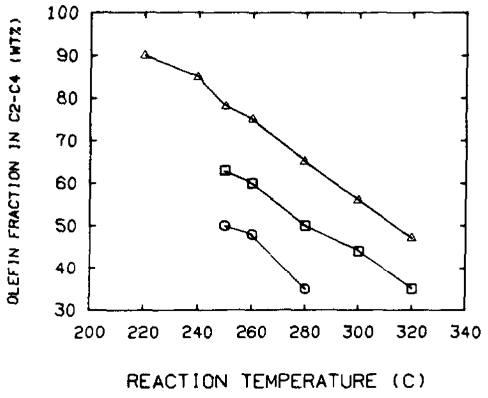

FIG. 9. Reaction temperature effect on selectivity for olefins (reaction conditions: 1 atm, $H_2/CO = 1$, GHSV = 1800). (□) I.E. (○) I.W. (△) V.I.

The same activation energies noted in Fig. 7 and Table 2 for these three catalysts indicate that diffusion effects were not significant in this study at any temperature.

Reduction temperature effects. The influence of the reduction temperature on the activity is shown in Fig. 10. For the ion-exchanged catalysts, the activity decreases slightly with increasing reduction temperature. This has been attributed by Jacobs *et al.* (*49*) to the sintering of the metal particles. The lower activity at 250°C is probably due to an incomplete reduction.

Contrary to the results found for the ion-exchanged catalysts, the activity for the incipient-wetness catalysts increased with increasing reduction temperature. This may

TABLE 2

Preparation Effects on Activation Energy

Prep. method	Ru (wt%)	Initial[a] E_{act} (kcal/mol)	Steady state[b] E_{act} (kcal/mol)
Incipient wetness	2	21	24
Ion exchange	3	16.7	23
Vapor impregnation	1	15.8	22

[a] 5 min after start of reaction.

[b] 30 min after start of reaction.

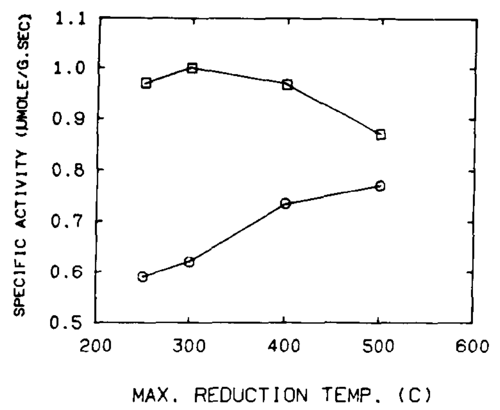

FIG. 10. Reduction temperature effect on specific activity (reaction conditions: 250°C, 1 atm, $H_2/CO = 1$, GHSV = 1800). (□) I.E. (○) I.W.

be due to an effect of residual chlorine. XPS and SIMS studies on unsupported Ru and FeRu alloys have shown that Ru metal indeed retains substantial amounts of chlorine after reduction of $RuCl_3$ to the metal (*50*). Koopman *et al.* (*51*) have examined the effect of reduction temperature on $RuCl_3/SiO_2$ and have found the metal surface area to be increased at higher temperatures due to the removal of traces of chlorine from the Ru surface. This would result in an increased specific activity following higher reduction temperatures.

Catalyst stability. In the reaction temperature range 200–300°C, it was found that the activities and selectivities are reproducible when going up and down with the temperature on using the hydrogen bracketing technique. Carbon deposition was also found to be reversible in that the carbon deposited at high temperatures could be hydrogenated at lower temperatures and vice versa.

Catalyst life tests for Ru/NaY were performed and are plotted in Fig. 11. All catalysts were very stable and suffered only a slight decrease in the first 30 min of reaction. Accompanying activity loss, selectivity shifted to higher hydrocarbons as shown in Fig. 12. After 30 h of continuous reaction, the catalysts were hydrogen treated at the reaction temperature and the experiment repeated. The phenomena described in Figs. 11 and 12 were thus found to be completely reproducible. This is in excellent agreement with the results reported by Dautzenberg *et al.* (*52*) for Ru/Al_2O_3 and Nijs and Jacobs (*41*) for ion-exchanged Ru/NaY. These results indicated that the selec-

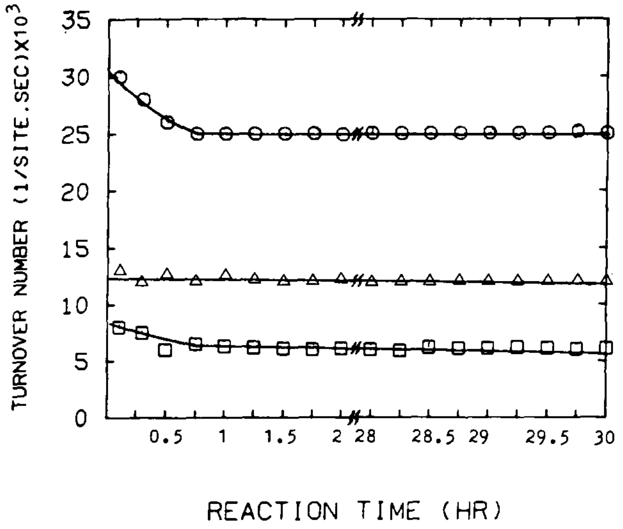

FIG. 11. Stability of Ru/NaY catalyst (reaction conditions: 250°C, 1 atm, $H_2/CO = 1$, GHSV = 1800). (□) I.E. (○) I.W. (△) V.I.

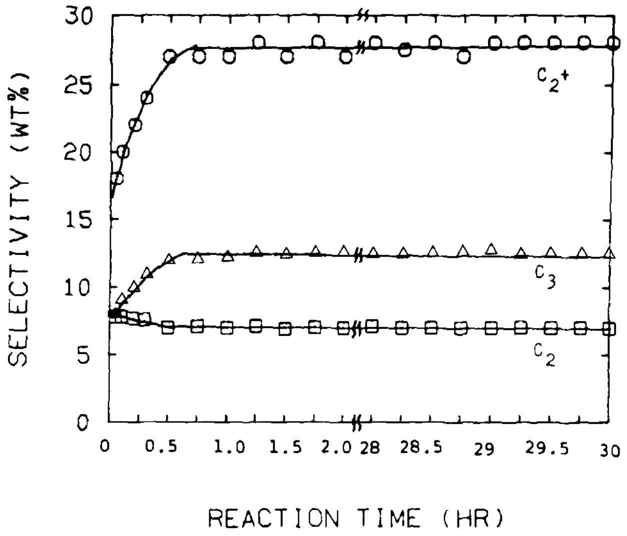

FIG. 12. Effect of reaction time on selectivity over 3% RuNaY (I.E.) catalysts. (reaction conditions: 250°C, 1 atm, $H_2/CO = 1$, GHSV = 1800).

tivity shift to higher hydrocarbons with reaction time is not due to the sintering of Ru metal. Nijs and Jacobs (*41*) concluded that at the beginning of FT synthesis some surface carbon is formed which is easily hydrogenated to methane but which does not initiate chain growth. Another species is gradually formed later on which can initiate chain growth. The rate at which this species is formed decreases when the catalyst support is more acidic. The formation of this second species is enhanced by the presence of water. The difference in activation energies between initial and steady state found here (Table 2) possibly suggests that slightly different reaction mechanisms may exist, i.e., as a result of an increase in water present, since little deactivation is seen.

CONCLUSIONS

The results presented in this study indicate that, using different preparation techniques, one is able to change greatly the chemical and physical properties of Ru/NaY catalysts. The CO/H ratio had a value of 2–3 for chemisorption on vapor-impregnated catalysts at ambient temperature, while the CO/H ratio of ion-exchanged catalysts had a value of 4–5 for average Ru particle diameters less than 1.6 nm. This ratio decreased rapidly as particle size increased. The CO/H ratio for the incipient-wetness catalysts was independent of average particle size in the range above 5 nm and had a value of about 1.5. These modifications in the nature and stoichiometry of CO and H_2 adsorption occur presumably because of different site geometries and/or the interaction of the metal with the zeolite.

The specific activity of supported ruthenium prepared by the ion-exchange method was found to increase with increasing average metal particle size in the range 1–3 nm. For the incipient-wetness catalysts specific activity was constant as average particle size varied above 3 nm. Catalysts prepared by the vapor-impregnation method exhibited a much higher activity than ion-exchanged catalysts having similar average particle sizes. A general pattern is evident, namely, increasing specific activity with decreasing CO/H adsorption ratio, suggesting that the relative availability of adsorbed H_2 and CO determines catalyst activity during reaction.

Selectivity in CO/H_2 reaction over Ru/NaY was influenced by the preparation method and metal loading. Selectivity for methane decreased with increasing metal loading for the ion-exchanged catalysts. This was less true for the catalysts prepared by the incipient-wetness technique, which had an anomalously high methane selectivity. The vapor-impregnated catalysts exhibited much higher selectivities for C_2–C_4 olefins and higher hydrocarbons than the other two catalysts.

It is hypothesized that, for ion-exchanged catalysts, partial migration of electronic charge from the metal atom to the proton of strongly acidic OH groups lead to the formation of a charge-transfer complex. Possibly, because of the presence of these acid sites in the ion-exchanged catalysts, isobutane is also able to be formed. As a result of the neutralization of the zeolite structure by only Na^+ cations in vapor-impregnated catalysts, the electron-deficient character of Ru in those catalysts appears to be negligible. Catalysts prepared by the incipient-wetness method have the same electronic state of the Ru as bulk metal since they have large Ru particles located on the external zeolite surface which apparently do not interact with the zeolite. It is interesting to note that the catalysts containing Ru highly dispersed, and in large part inside the zeolite structure (ion-exchanged and vapor-impregnated catalysts), have the best selectivities for higher hydrocarbons. Considering the case of the vapor-impregnated catalysts, this selectivity for higher hydrocarbons should not be due only to a strong metal–zeolite interaction.

On the basis of this and previous studies, it appears that the observed changes in adsorption, activity, and selectivity with preparation method and metal dispersion are probably the result of differences in the location of the metal, average metal particle size, and interaction between the metal and the zeolite.

ACKNOWLEDGMENTS

Financial support for this study was provided by the U.S. Department of Energy, Office of Fossil Energy, under Grant DE-FG22-81PC40774.

REFERENCES

1. Vannice, M. A., *J. Catal.* **37,** 449 (1975).
2. Goodwin, J. G., and Naccache, C., *J. Mol. Catal.* **14,** 259 (1982).
3. Gallezot, P., Coudurier, G., Primet, M., and Imelik, B., *in* "Molecular Sieves II" (J. R. Katzer, Ed.), Vol. 40, p. 144. ACS Symposium Series, 1977.
4. Fabec, J. L., *Atomic Spec.* **4,** 46 (1983).
5. Benson, J. E., and Boudart, M., *J. Catal.* **4,** 704 (1965).
6. Wilson, G. R., and Hall, W. K., *J. Catal.* **17,** 190 (1970).
7. Payne, V. L., Ph.D. thesis, University of Illinois at Urbana-Champaign, 1982.
8. Yang, C.-H., and Goodwin, J. G., Jr., *React. Kinet. Catal. Lett.* **20,** 13 (1982).
9. Vannice, M. A., and Garten, R. L., *J. Catal.* **63,** 255 (1980).
10. Dalla Betta, R. A., *J. Catal.* **34,** 57 (1974).
11. Elliott, D. J., and Lunsford, J. H., *J. Catal.* **57,** 11 (1979).
12. Gustafson, B. L., and Lunsford, J. H., *J. Catal.* **74,** 393 (1982).
13. Pederson, L. A., and Lunsford, J. H., *J. Catal.* **61,** 39 (1980).
14. Pearce, J. R., Mortier, W. J., and Uytterhoeven, J. B., *J. Chem. Soc. Faraday Trans. 1* **75,** 1395 (1979).
15. Verdonck, J. J., Jacobs, P. A., Gent, M., and Poncelet, G., *J. Chem. Soc. Faraday Trans. 1* **76,** 403 (1980).
16. Goodwin, J. G., Jr., unpublished results.
17. Kellner, C. S., and Bell, A. T., *J. Catal.* **71,** 296 (1981).
18. Clausen, C. A., III, and Good, M. L., *J. Catal.* **38,** 92 (1975).
19. Chukin, G. D., Laundau, M. V., and Druglikov, V. Y., *in* "Proceeding, 6th International Congress on Catalysis" (G. C. Bond, P. B. Wells, and F. C. Tompkins, Eds.), p. 688. The Chemical Society, London, 1977.
20. Cusumano, J. A., Dalla Betta, R. A., and Levy, R. B., "Catalysis in Coal Conversion," p. 32. Academic Press, New York, 1978.
21. Kobayashi, M., and Shirasaki, T., *J. Catal.* **28,** 289 (1978).
22. Dalla Betta, R. A., *J. Phys. Chem.* **79,** 2519 (1975).
23. Wang, H.-T., Chen, Y.-W., and Goodwin, J. G., Jr., *Zeolites,* in press.
24. Goodwin, J. G., Jr., and Naccache, C., *J. Catal.* **64,** 482 (1980).
25. Goodwin, J. G., Jr., and Naccache, C., *Appl. Catal.* **4,** 145 (1982).
26. Sheppard, N., and Nguyen, T. T., *in* "Advances in Infrared and Raman Spectroscopy" (R. J. H. Clark and R. E. Hester, Eds.), Vol. 5, Chap. 2, p. 66. Heyden.

27. Blackmond, D. G., and Goodwin, J. G., *J. Chem. Soc. Chem. Commun.* 125 (1981).
28. Ekerdt, J. G., and Bell, A. T., *J. Catal.* **58,** 170 (1979).
29. Kuzentsov, V. L., and Bell, A. T., *J. Catal.* **65,** 374 (1980).
30. Yamaski, H., Kobori, Y., Naito, S., Onishi, T., and Tamaru, K., *J. Chem. Soc. Faraday Trans. 1* **77,** 2913 (1981).
31. Dalla Betta, R. A., *J. Phys. Chem.* **79,** 2519 (1975).
32. Brown, M. F., González, R. D., *J. Phys. Chem.* **80,** 1731 (1976).
33. Kellner, C. S., and Bell, A. T., *J. Catal.* **75,** 251 (1982).
34. Bossi, A., Garbassi, F., Petrini, G., and Zanderighi, L., *J. Chem. Soc. Faraday Trans. 1* **78,** 1029 (1982).
35. Vedrine, J. C., Dufaux, M., Naccache, C., and Imelik, B., *J. Chem. Soc. Faraday Trans. 1* **74,** 440 (1978).
36. Shyu, J. Z., Hercules, D. M., and Goodwin, J. G., Jr., manuscript in preparation.
37. King, D. L., *J. Catal.* **51,** 386 (1978).
38. Jacobs, P. A., *in* "Catalysis by Zeolites" (B. Imelik, C. Naccache, Y. Ben Taarit, J. C. Vedrine, G. Coudurier, and H. Praliaud, Eds.), p. 293, Elsevier, Amsterdam, 1980.
39. Jung, H. J., Ph.D. thesis, The Pennsylvania State University, 1981.
40. Bartholomew, C. H., Pannell, R. B., and Butler, J. L., *J. Catal.* **65,** 335 (1980).
41. Nijs, H. H., and Jacobs, P. A., *J. Catal.* **66,** 401 (1980).
42. Chen, Y. W., Wang, H. T., and Goodwin, J. G., Jr., *J. Catal.*, in press.
43. Goodwin, J. G., Jr., Chen, Y. W., and Wang, H. T., "Site Activities of Zeolite-Supported Ru for CO hydrogenation." 4th Quarterly Report, DOE, January 1982.
44. Amelse, J. A., Schwartz, L. H., and Butt, J. B., *J. Catal.* **72,** 95 (1981).
45. Kellner, C. S., and Bell, A. T., *J. Catal.* **67,** 175 (1981).
46. Kellner, C. S., and Bell, A. T., *J. Catal.* **70,** 418 (1981).
47. Castner, D. G., Blackadar, R. L., and Somorjai, G. A., *J. Catal.* **66,** 257 (1980).
48. Biloen, P., private communication.
49. Jacobs, P. A., Nijs, H. H., Verdonck, J. V., and Uytterhoeven, J. B., *Prepr. Div. Pet. Chem. Am. Chem. Soc.* **23,** 469, (1978).
50. Ott, G. L., Delgass, W. N., Winogard, N., and Baltinger, W. E., *J. Catal.* **56,** 174 (1979).
51. Koopman, P. G. T., Kieboom, A. P. G., and van Bekkum, H., *J. Catal.* **69,** 172 (1981).
52. Dautzenberg, F. N., Helle, J. N., Van Santen, R. A., and Verbeek, H., *J. Catal.* **50,** 8 (1977).